SEMARAK ILMU PUBLISHING

CFD Letters

Journal homepage:
https://semarakilmu.com.my/journals/index.php/CFD_Letters/index
ISSN: 2180-1363

Effects of Activation Energy and Diffusion Thermo an Unsteady MHD Maxwell Fluid Flow over a Porous Vertical Stretched Sheet in the Presence of Thermophoresis and Brownian Motion

Aruna Ganjikunta[1], Bhagya Lakshmi Kuntumalla[2], Ramachandra Reddy Vaddemani[3,*]

[1] Department of Mathematics, GITAM University, Hyderabad, Telangana, Pincode- 502329, India
[2] Department of Mathematics, CMR Technical Campus, Kandlakoya (village), Medchal, Hyderabad, Telangana, Pincode-500059, India
[3] Department of Humanities and Sciences, K.S.R.M College of Engineering, Kadapa, Aandra Pradesh, Pin-516005, India

ARTICLE INFO

Article history:
Received 24 July 2023
Received in revised form 21 August 2023
Accepted 20 September 2023
Available online 31 July 2024

Keywords:
Mixed convective flow; Maxwell fluid; nonlinear thermal radiation; porous sheet

ABSTRACT

This article discusses the effects of Activation energy and Diffusion thermo on an unsteady MHD flow of an electrically conducting Maxwell Nanofluid over a stretching sheet in a porous medium in the presence of thermophoresis and Brownian motion. Using the similarity transformations, the partial differential equations corresponding to the momentum, energy, and concentration equations are transformed into a system of nonlinear ordinary differential equations, which are solved numerically using a RungeKutta fourth-order method along with the shooting technique, and the results obtained for different governing flow parameters are drawn graphically, and their effects on velocity, temperature, and concentration profiles are discussed. The values of the skin friction coefficient, Nusselt number coefficient, and Sherwood number coefficient are presented in the table. A comparison with previously reported data is made, and an excellent agreement is noted. The objective of the present study is to use the Activation energy and Diffusion thermo parameters to increase the concentration of chemical species on the boundary layer and temperature, respectively. The temperature of the fluid increases as the radiation parameter, Brownian motion, thermophoresis, and magnetic parameters increase.

1. Introduction

The growing trend in technical and industrial applications grabs the attention of researchers to analyse mathematical models for non-Newtonian fluids. There are various applications of non-Newtonian liquids such as in metal extrusion, spinning of metals, lubricant manufacturing for multiple vehicles, the distillation of molten metal from non-metallic insertion, manufacturing of shoes (to protect feet from injuries, the shoe needs to be packed with a specific non-Newtonian fluid), and food and medicine industries, and as a coolant. With the passage of time, various researchers have presented mathematical models of non-Newtonian fluids for analyzing the characteristics of these fluids.

* *Corresponding author.*
E-mail address: vrcreddymaths77@gmail.com (Ramachandra Reddy Vaddemani)

https://doi.org/10.37934/cfdl.16.12.1837

Maxwell was the first to model a non-Newtonian fluid; its examples include polymer extrusion, nuclear reactor emergency cooling systems, food processing, and thermal welding. As the authors know, Maxwell fluid's steady-state boundary layer flow across a porous flat plate with the above-mentioned physical consequences has yet to be documented in the literature. Many authors have conducted a study using different geometries and parameters. But they have yet to study a porous flat plate combining thermal radiation, MHD, and heat generation over a Maxwell fluid flow with a moving velocity in the boundary condition. The Maxwell model is one such important subclass of mathematical models. Various researchers apply this model under different flow circumstances. Zierep and Fetecau [1] analyzed the energetic balance for Rayleigh–Stokes's first and second problems of the Maxwell fluid under the effect of various initial and boundary conditions. Fetecau *et al.,* [2] also presented an unsteady flow for the Maxwell fluid of fractional derivatives under the influence of an accelerating plate with constant speed. In this examination, they solved the modeled equations by employing a combination of joint Fourier sine, and Laplace transforms and discussed various cases for the flow system. Renardy and Wang [3] addressed the boundary layer flow for the Maxwell fluid. In this study, these authors investigated that the boundary layer is basically of two types: the stress boundary layer and the Prandtl boundary layer. Accordingly, Raghunath *et al.,* [4] have studied unsteady magneto-hydro-dynamics flow of Jeffrey fluid through porous media with thermal radiation, Hall current and Soret effects. Raghunath *et al.,* [5] have reviewed processing to pass unsteady MHD flow of a second-grade fluid through a porous medium in the presence of radiation absorption exhibits Diffusion thermo, hall and ion slip effects. Suresh Kumar *et al.,* [6] have possessed Numerical analysis of magnetohydrodynamics Casson nanofluid flow with activation energy, Hall current and thermal radiation. Omar *et al.,* [7] have expressed Hall Current and Soret Effects on Unsteady MHD Rotating Flow of Second-Grade Fluid through Porous Media under the Influences of Thermal Radiation and Chemical Reactions. Deepthi *et al.,* [8] have reviewed Recent Development of Heat and Mass Transport in the Presence of Hall, Ion Slip and Thermo Diffusion in Radiative Second Grade Material: Application of Micromachines. Aruna *et al.,* [9] have analyzed an unsteady MHD flow of a second-grade fluid passing through a porous medium in the presence of radiation absorption exhibits Hall and ion slip effects. Raghunath and Mohanaramana [10] have discussed Hall, Soret, and rotational effects on unsteady MHD rotating flow of a second-grade fluid through a porous medium in the presence of chemical reaction and aligned magnetic field.

Radiation is the energy transfer from a body via electromagnetic radiation emission or absorption. Thermal radiation spreads in the absence of substances through the vacuum of space. In contrast to conduction and convection, heat radiation can be concentrated in a limited area using reflecting mirrors, which produce focused solar energy. Raghunath *et al.,* [11] have discussed Hall and ion slip radiative flow of chemically reactive second grade through porous saturated space via perturbation approach. From their result, it can be seen that temperature distribution and thermal boundary layer reduce with an increase of dimensionless thermal free convection parameter, dimensionless mass free convection parameter, and Prandtl number. According to the research by Ramachandra *et al.,* [12] have possessed Effects of Hall Current, Activation Energy and Diffusion Thermo of MHD Darcy-Forchheimer Casson Nanofluid Flow in the Presence of Brownian Motion and Thermophoresis. Hsiao [13] described a thermal extrusion system that combines electrical MHD heat transfer with Maxwell fluid, considered radiative and viscous dissipation. In the above research, the authors have used radiation and heat generation in other fluids that flow on a flat porous medium. Reddy *et al.,* [14] published the outcomes of a numerical computation study on how thermal outlines along the side walls of an annular enclosure made up of various hybrid nanofluids with insulated horizontal borders are affected by axially variable temperature.

Thermo-diffusion is a transport process in which the particles are transported to a mixture of several factors determined through the temperature gradient. As heat and mass transfer occurs in fluid motion, the driving potential and flow resistance become more complex. This results in a continuous difference within the concentration of one species in the chemical process relative to the other species. Thanks to its wide range of applications in heat exchangers for packed beds, heat insulation, energy storage devices, drying technology, nuclear waste repositories, catalytic reactors, and geothermal systems, the mass and heat transport in porous media is further enhanced by investigations experimentally and theoretically. VenkataRamudu *et al.,* [15] have studied Heat and mass transfer in MHD Cassonnanofluid flow past a stretching sheet with thermophoresis and Brownian motion. Cheng [16] examined the impacts of Dufour and Soret of a heated plate on viscous liquid flow. Hayat *et al.,* [17] considered the impacts of Dufour and Soret on the stretching sheet of the hyperbolic tangent fluid. Hayat *et al.,* [18] examined the variation in diffusionthermal and thermal-diffusion within the convective flow to the stretching layer of a second-grade liquid. The thermal and mass transfer characteristics of the naturally produced convection on the vertical surface of the saturated porous substance linked to a magnetic field, considering Dufour and Soret effects, have been numerically investigated by Postelnicu [19]. Kafoussias and Williams [20] considered boundary layer streams for mixed forced-natural convection in the existence of Soret and Dufour related to thermodiffusion and diffusion-thermo effects.

The study of heat transfer with chemical reactions in the presence of nanofluids is of great practical importance to engineers and scientists because of its almost universal occurrence in many branches of science and engineering. Possible applications of this type of flow can be found in many industries. In many engineering applications such as nuclear reactor safety, combustion systems, solar collectors, metallurgy, and chemical engineering, many transport processes are governed by the joint action of the buoyancy forces from both thermal and mass diffusion in the presence of chemical reaction effects. Radiative flows are encountered in countless industrial and environmental processes such as heating and cooling chambers, fossil fuel combustion and energy processes, evaporation from sizeable open water reservoirs, astrophysical flows, and solar power technology. However, the thermal radiation heat transfer effects on different flows are significant in high-temperature processes and space technology. Thermophoresis is the change in position/migration of the large structure molecules to a macroscopic temperature gradient. The phenomenon is observed due to the exhibition of different responses of particles. Raghunath *et al.,* [21] have studied Diffusion Thermo and Chemical Reaction Effects on Magnetohydrodynamic Jeffrey Nanofluid over an Inclined Vertical Plate in the Presence of Radiation Absorption and Constant Heat Source. Raghunath [22] has studied Study of Heat and Mass Transfer of an Unsteady Magnetohydrodynamic Nanofluid Flow Past a Vertical Porous Plate in the Presence of Chemical Reaction, Radiation and Soret Effects. . Raghunath *et al.,* [23] have discussed Unsteady MHD fluid flow past an inclined vertical porous plate in the presence of chemical reaction with aligned magnetic field, radiation, and Soret effects. Raghunath *et al.,* [24] have possessed Characteristics of MHD Casson fluid flow past an inclined vertical porous plate. Raghunath *et al.,* [25] have expressed Effects of Radiation Absorption and Aligned Magnetic Field on MHD Cassion Fluid Past an Inclined Vertical Porous Plate in Porous Media. Raghunath *et al.,* [26] have studied Influence of MHD mixed convection flow for maxwell nanofluid through a vertical cone with porous material in the existence of variable heat conductivity and diffusion.

The principal aim of the present work is to study the impacts of Activation energy and diffusion thermo on unsteady MHD Maxwell fluid flow past a porous, vertically stretching sheet in the presence of thermophoresis and Brownian motion. The governing equations can obtain similarity transformations that reduce a system of governing partial differential equations and associated

boundary conditions to a system of ordinary differential equations. This transformation derives third- and second-order ordinary differential equations corresponding to momentum, energy, and concentration equations. These equations are solved with the help of RungeKutta's fourth order and shooting technique. The effects of different flow parameters on velocity, temperature, and concentration profiles are investigated and analyzed with the help of a graphical representation.

2. Problem Formulation

We consider 2D viscous incompressible laminar flow with heat transmission of a non-Newtonian electrically conducting Maxwell Nanofluid through a porous medium and also the combined effects of mixed convection with convective boundary conditions. Flow is considered on a stretching sheet in the presence of Dufour and Soret effects and variable thermal conductivity. A uniform magnetic field $B = \frac{B_0}{\sqrt{1-\chi t}}$ is applied in opposite to the direction of the fluid flow. The stretched sheet of velocity is $U_w = \frac{cx}{\sqrt{1-\chi t}}$ and $v = v_w = \frac{v_0}{\sqrt{1-\chi t}}$ where c, χ are positive constants. In addition, all physical attributes related to the formula are measured to be constant. The geometry of this modelling can be displayed in Figure 1. Bossineq approximation is taken for both energy or temperature and concentration profiles. The continuity, momentum, energy and concentration equations governing such type of flow in the presence of chemical reaction are written as below:

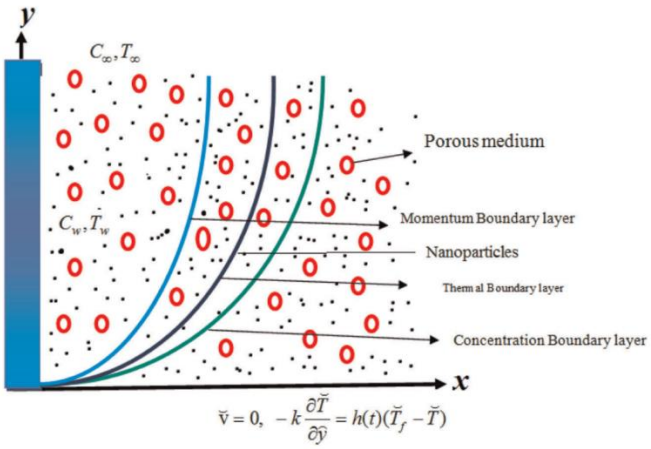

Fig. 1. Physical configuration of the problem

$$\frac{\partial u}{\partial x} + \frac{\partial u}{\partial y} = 0 \tag{1}$$

$$\frac{\partial u}{\partial t} + u\frac{\partial u}{\partial x} + v\frac{\partial u}{\partial y} = \nu\frac{\partial^2 u}{\partial y^2} - \lambda_1\left(u^2\frac{\partial^2 u}{\partial x^2} + v^2\frac{\partial^2 u}{\partial y^2} + 2uv\frac{\partial^2 u}{\partial x\,\partial y}\right) + g\beta_T(T - T_\infty) + g\beta_C(C - C_\infty) - \sigma\frac{B_0(t)}{\alpha} - \frac{\vartheta}{k}u \tag{2}$$

$$\frac{\partial T}{\partial t}+u\frac{\partial T}{\partial x}+v\frac{\partial T}{\partial y}=\alpha_m\left(\frac{\partial^2 T}{\partial y^2}\right)+\tau\left(D_B\frac{\partial C}{\partial y}\frac{\partial T}{\partial y}+\frac{D_T}{T_\infty}\left(\frac{\partial T}{\partial y}\right)^2\right)-\frac{1}{(\rho Cp)}\frac{\partial q_r}{\partial y}+\frac{\mu}{(\rho c)_f}\left(\frac{\partial u}{\partial y}\right)^2+\frac{D_m k_T}{c_s c_p}\frac{\partial^2 C}{\partial y^2} \tag{3}$$

$$\frac{\partial C}{\partial t}+u\frac{\partial C}{\partial x}+v\frac{\partial C}{\partial y}=D_B\left(\frac{\partial^2 C}{\partial y^2}\right)+\frac{D_T}{T_\infty}\left(\frac{\partial T^2}{\partial y^2}\right)--k_r^2(C-C_\infty)\left(\frac{T}{T_\infty}\right)^m\exp\left(\frac{-E_a}{K^*T}\right) \tag{4}$$

For this flow, corresponding boundary conditions are

$$\begin{aligned} &u=U_w(x,t),\quad v=0,\ -k\frac{\partial T}{\partial y}=h(t)(T_f-T_\infty),\ \ C=C_w \quad \text{at } y=0\\ &u\to 0,\quad v\to 0,\ \ T\to T_\infty \qquad C\to C_\infty \qquad\qquad \text{as } y\to\infty \end{aligned} \tag{5}$$

Where (u,v) are the components of velocity in x and y directions, λ_1 is the relaxation time, υ is the kinematic viscosity, κ_0 is the chemical reaction parameter, g is the gravitational acceleration, β_T is the thermal expansion coefficient, (T,C) are fluid temperature and concentration, and DB and DT are Brownian and thermophoretic coefficient, the density of the fluid.

The radiative heat flux q_r (using Roseland approximation followed [24]) is defined as

$$q_r=-\frac{4\sigma^*}{3k^*}\frac{\partial T^4}{\partial y} \tag{6}$$

Where k^* is the mean absorption coefficient, and $\sigma^*$is the Stefan-Boltzmann constant.

We assume that the temperature variances inside the flow are such that the term T^4 can be represented as linear function of temperature. This is accomplished by expanding T^4 in a Taylor series about a free stream temperature T_∞ as follows:

$$T^4=T_\infty^4+4T_\infty^3(T-T_\infty)+6T_\infty^2(T-T_\infty)^2+\ldots\ldots\ldots \tag{7}$$

After neglecting higher-order terms in the above equation beyond the first degree term in $(T-T_\infty)$, we get

$$T^4\cong 4T_\infty^3T-3T_\infty^4 \tag{8}$$

Using Eq. (8) in Eq. (6) and then the substitution of its value in Eq. (3), gives

$$\frac{\partial q_r}{\partial y}=-\frac{16\sigma^*T_\infty^3}{3k^*}\frac{\partial^2 T}{\partial y^2} \tag{9}$$

Using Eq. (9), Eq. (3) can be written as

$$\frac{\partial T}{\partial t}+u\frac{\partial T}{\partial x}+v\frac{\partial T}{\partial y}=\alpha_m\left(\frac{\partial^2 T}{\partial y^2}\right)+\tau\left(D_B\frac{\partial C}{\partial y}\frac{\partial T}{\partial y}+\frac{D_T}{T_\infty}\left(\frac{\partial T}{\partial y}\right)^2\right)-\frac{1}{(\rho c)_f}\frac{16T_\infty^3\sigma^*}{\partial K^*}\left(\frac{\partial^2 T}{\partial y^2}\right)+\frac{\mu}{(\rho c)_f}\left(\frac{\partial u}{\partial y}\right)^2+\frac{D_m k_T}{c_s c_p}\frac{\partial^2 C}{\partial y^2} \tag{10}$$

The following similarity variables are introduced for solving governing Eq. (2), Eq. (6) and Eq. (4) as

$$u=\frac{ax}{1-\chi t}f'(\eta),\ v=-\sqrt{\frac{a}{(1-\chi t)}}f(\eta),\ \eta=\sqrt{\frac{va}{1-\chi t}}y,\ \phi(\eta)=\frac{C-C_\infty}{C_w-C_\infty},$$

$$\theta(\eta)=\frac{T-T_\infty}{T_w-T_\infty},h(t)=\frac{d}{\sqrt{1-\chi t}}. \tag{11}$$

Substituting Eq. (11) into Eq. (2), Eq. (3) and Eq. (4), we get the following system of non-linear ordinary differential equations

$$f'''-f'^2+ff''+\Lambda\left(2ff'f''-f^2f'''\right)-\delta\left(f'+\frac{1}{2}\eta f''\right)-(M+\beta)f'+\lambda(\theta+N\phi)=0 \tag{12}$$

$$\left(1+\frac{4}{3}R_d\right)\theta''-\delta\,\mathrm{Pr}\frac{1}{2}\eta\theta'-\mathrm{Pr}\,f\theta'+\mathrm{Pr}\,N_b\left(\theta'\phi'+\frac{N_t}{N_b}\theta'^2\right)-E_c f''+\mathrm{Pr}\,D_u\phi'=0 \tag{13}$$

$$\phi''-\delta\,\mathrm{Pr}\frac{1}{2}\eta\phi'-Scf\phi'+\frac{N_b}{N_t}\theta''-K_E(1+\theta)^m\varphi\exp\left(\frac{-E}{1+\theta}\right)=0 \tag{14}$$

The corresponding boundary conditions Eq. (5) become;

$$\begin{aligned}&f(\eta)=S,\quad f'(\eta)=1,\quad \theta'(\eta)=-\gamma(1-\theta(\eta)),\quad \phi(\eta)=1 \qquad at \quad \eta=0\\ &f'(\eta)\to 0,\quad \theta(\eta)\to 0,\quad \phi(\eta)\to 0 \qquad as \quad \eta\to\infty\end{aligned} \tag{15}$$

Where prime denotes differentiation with respect to η, and the significant thermophysical parameters indicating the flow dynamics are defined by

$\delta=\frac{c}{\chi}$ is the Unsteady Parameter,

$\Lambda=c\lambda_1$ is the Maxwell fluid parameter,

$\lambda = \left(\frac{g\beta_T (T_w - T_\infty)x}{U_w^2} \right)$ is the mixed convection parameter

$N = \frac{\beta_c (C_w - C_\infty)}{\beta_T (T_w - T_\infty)}$ is the Deborah Number

$\beta = c\lambda_1$ is the dimensionless bouncy parameter

$M = \frac{\sigma B_0^2}{\rho Cp}$ is the magnetic number

$N_b = \frac{\tau D_B (C_w - C_\infty)}{\nu}$ is the Brownian motion parameter

$N_t = \frac{\tau D_T (T_w - T_\infty)}{\alpha}$ is the thermophoresis parameter

$R_d = \frac{4\sigma^* T_\infty^3}{kk^*}$ is the radiation parameter

$\Pr = \frac{\nu}{\alpha} = \frac{\nu \rho C_p}{k}$ is the Prandtl number

$Sc = \frac{\nu}{D_B}$ is the Schmidt number

$\gamma = \left(\frac{h_f}{k} \sqrt{\frac{\nu}{\alpha}} \right)$ is the Biot number

$E_c = \frac{U_w^2}{C_p (T_w - T_\infty)}$ is the Eckert number

$K_E = \frac{k_r^2}{c}$ is the rate of chemical reaction parameter

$Du = \frac{D_M k_T (C_w - C_\infty)}{C_S C_p \nu a^2 (T_w - T_\infty)}$ is the Diffusion thermo parameter

$E = \frac{E_a}{K^* T_\infty}$ is the Activation energy parameter

The local skin friction coefficient Cf, the local Nusselt number Nu_x, and the local Sherwood number Sh_x are the physical quantities of relevance that influence the flow. These numbers have the following definitions:

$$C\,f = \frac{\tau_w}{\rho U_w^2},\quad Nu_x = \frac{x q_w}{k\left(T_w - T_\infty\right)},\quad Sh_x = \frac{x\,q_m}{D_B\left(C_w - C_\infty\right)} \tag{16}$$

The shear stress, heat, and mass flux are written as

$$\tau_w = \mu\left[\frac{\partial u}{\partial y}\right]_{y=0},\quad q_w = -k\left[\frac{\partial T}{\partial y}\right]_{y=0},\quad q_m = D_B\left[\frac{\partial C}{\partial y}\right]_{y=0} \tag{17}$$

The coefficient of skin friction, the Nusselt number, and the Sherwood number are all expressed in their non-dimensional versions in terms of the similarity variable as follows:

$$\mathrm{Re}_x^{1/2}\,Cf = f''(0),\quad \mathrm{Re}_x^{-1/2}\,Nu_x = -\left(1+\frac{4}{3}R_d\right)\theta'(0),\quad \mathrm{Re}_x^{-1/2}\,Sh_x = -\phi'(0) \tag{18}$$

3. Solution Methodology

As Eq. (12) – Eq. (14) with boundary conditions Eq. (15) are strongly non-linear, it is difficult or maybe impossible to find the closed form solutions. Accordingly, these boundary value problems are solved numerically by using the conventional fourth-order RK integration scheme along with the shooting technique.

The first task to carry out the computation is to convert the boundary value problem to an initial value problem.

Let by using the following notations:

$$f = y_1,\ f' = y_2,\ f'' = y_3,\ f''' = y_3',\ \theta = y_4,\ \theta' = y_5, \theta'' = y_5',\ \phi = y_6,\ \phi' = y_7, \phi'' = y_7'. \tag{19}$$

By using the above variables, the system of first-order ODEs is

$$y_1' = y_2, \tag{20}$$

$$y_2' = y_3, \tag{21}$$

$$y_3' = \frac{1}{\left(1+\Lambda y_1^2\right)}\left(y_2^2 - y_1 y_3 - 2\Lambda y_2 y_3 + \delta\left(y_2 + \frac{1}{2}n y_3\right) + \left(M+\beta\right)y_2 - \lambda\left(y_4 + N y_6\right)\right), \tag{22}$$

$$y_4' = y_5, \tag{23}$$

$$y_5' = \frac{1}{1+R_d}\left(\frac{1}{2}\delta\eta \,\mathrm{Pr}\, y_5 + \mathrm{Pr}\, y_1 y_5 - \mathrm{Pr}\, N_b\left(y_5 y_7 + \frac{Nt}{Nb}(y_5)^2\right) + Ecy_3 - \mathrm{Pr}\ Du\, y_7\right) \tag{24}$$

$$y_6' = y_7, \tag{25}$$

$$y_7' = \frac{1}{2}\delta\eta \,\mathrm{Pr}\, y_7 + Scy_1 y_7 - \frac{N_b}{N_t} y_5' + y_4 K_E (1+y_4)^m \exp\left(\frac{-E}{1+y_6}\right) \tag{26}$$

The boundary conditions are given as

$$\begin{aligned} &y_1(0) - S = 0, \quad y_2(0) - 1 = 0, \quad y_5(0) + \gamma(1 - y_4(0)) = 0, \quad y_6(0) - 1 = 0 \\ &y_2(\infty) = 0, \quad y_4(\infty) = 0, \quad y_6(\infty) = 0 \end{aligned} \tag{27}$$

The boundary conditions in Eq. (27) are utilized via use a finite value of η_{max} as given

$$f'(\eta_{\max}) \to 0,\ \theta'(\eta_{\max}) \to 0,\ \phi'(\eta_{\max}) \to 0. \tag{28}$$

The step is taken $\Delta\eta = 0.001$ and convergent criteria is 10^{-6} for the desired accuracy

4. Code Validation

We checked the accuracy of current outcomes with previous literature in the limited case and obtained a fantastic agreement. Table 1 displays a comparison of numeric outcome for f"(0) numerous values of the magnetic field parameter with the published result of Venkata Ramudu *et al.,* [15] with an outstanding agreement.

5. Result and Discussion

In the current work, the MHD flow of Maxwell nanoparticles with convective boundary conditions is examined. Also, heat transfer and viscous dissipation are considered. To show the effect of some pertinent physical aspects, the obtained result is computed. The outcome of these physical parameters is elaborated through graph 2–22 and in Table 2, we computed the value of $\mathrm{Re}_x^{1/2} Cf_x$, $\mathrm{Re}_x^{-1/2} Nu_x$ *and* $\mathrm{Re}_x^{-1/2} Sh_x$ for entrenched flow variables.

For different values of the magnetic parameter M, the velocity and the temperature profiles are plotted in Figure 2 and 3 respectively. From Figure 2, it is clear that an increase in the magnetic parameter M leads to a fall in the velocity. The effects of the magnetic parameter to increase the temperature profiles are noticed from Figure 3. The presence of Lorentz force retards the force on the velocity field and therefore the velocity profiles decreases with the effect of magnetic parameter. This force has the tendency to slow down the fluid motion and the resistance offered to the flow. Therefore, it is possible for the increase in the temperature.

Figure 4 and Figure 5 are displayed to study the velocity f'(η), and temperature θ(η) profiles for the numeric value of porosity parameter β. It is observed that the velocity field is a declining function of porosity variable β. actually, a higher value of β causes a stronger restriction and growing thickness

of porous medium due to which the fluid flow motion depreciates. So, the velocity of the fluid reduces with an increased value of β. But, the opposite behavior is noted in θ (η).

The velocity f ′(η), temperature θ (η), and concentration ϕ (η), profiles for the diverse values of an unsteadiness parameter δ are evaluated in Figure 6 – Figure 8. It is seen that from Figures 6 and Figure 8, an increment in the value of δ obtains diminution in the velocity field and concentration distribution as the momentum and solute boundary layer. There is an increment in the temperature of nanoparticles via a larger value of δ as the thermal boundary layer.

The impact of fluid parameter ʌ for velocity f′(η), temperature field θ(η) and concentration of nanoparticles ϕ (η) is considered in Figure 9 – Figure 11. It is clearly noticed from these figures the waning function of the fluid parameter. It can be observed that the influence of enhancing the estimations of fluid parameters ε is to depreciate the f′(η), field and is associated with boundary layer thickness depreciating. The θ(η) and ϕ (η) both are showing as opposite behavior with increasing value of the fluid parameter.

Temperature is enhanced when the Brownian motion parameter Nb is increased. Larger the Brownian motion parameter, lower the viscous force and higher the Brownian diffusion coefficient which results an enhancement in the thermal boundary layer thickness and temperature and this phenomenon can be observed in Figure 12. From Figure 13, it is observed that the nanoparticle concentration decreases with an increment in Nb.

Figure 14 and Figure 15 illustrate the effect of thermophoresis parameter Nt on the temperature and the nanoparticles concentration profile. One can observe that temperature fields' increase with an enhancement in Nt. Thermophoresis parameter plays an important role in the heat transfer flow. Thermophoresis force enhances when Nt is increased which tends to move the nanoparticles from the hot region to the cold and as a result the temperature and the boundary layer thickness increase. The opposite behavior has observed in Figure 15, in the case of concentration field.

Figure 16 – Figure 17 illustrates the influence of the radiation parameter (Rd) on the temperature and concentration profiles. It is apparent that an increase in the radiation parameter results in a corresponding temperature rise. The observed phenomenon can be attributed to the liberation of heat energy into the fluid, consequent to increased thermal radiation. The phenomenon of reversal behavior has been observed in the field of concentration. The temperature field's effects, as influenced by the Eckert number Ec are presented in Figure 18. The augmentation of the Eckert number results in an elevation of the temperature field.

Figure 19 - Figure 20 depicts the effect of Dufour parameter on temperature and concentration profiles respectively. As the Dufour parameter increases, the energy or temperature and concentration profiles are increases. The Dufour number denotes the contribution of the concentration gradients to the thermal energy flux in the flow. It can be seen that an increase in the Dufour number causes a rise in temperature.

The influence of the activation energy (E) on the concentration field is seen in Figure 21. The graph demonstrates that the concentration profile rises as the value of E increases. The Arrhenius function degrades due to the activation energy snowballing value, which ultimately leads to the encouragement of the generative chemical reaction, which in turn causes an improvement in the concentration field. When the temperature is low and the activation energy is high, a lower reaction rate constant is produced, which causes the chemical reaction to proceed more slowly. Increased focus is the direct result of this strategy. Figure 22 demonstrates that an increase in the rate of chemical reaction (σ) causes a significant decrease in the concentration profile. A high chemical reaction rate causes a fallout solute boundary layer to become denser.

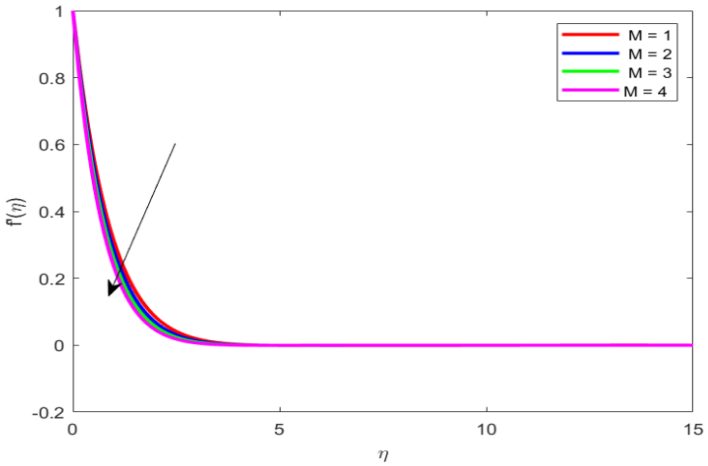

Fig. 2. Effect of magnetic parameter M on velocity profiles

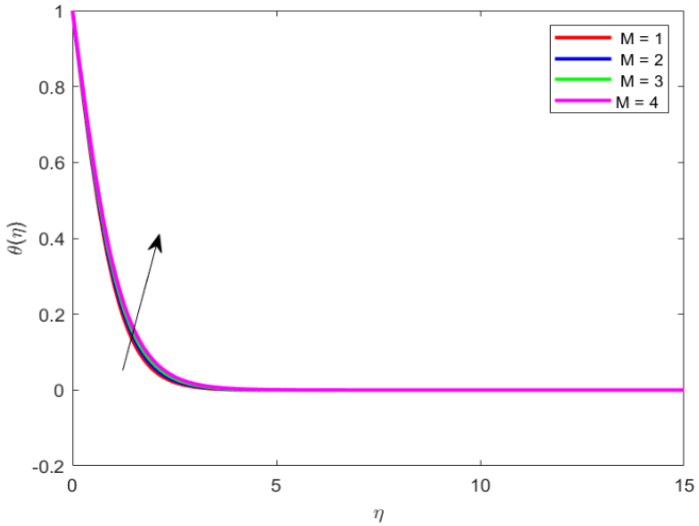

Fig. 3. Effect of M on temperature profiles

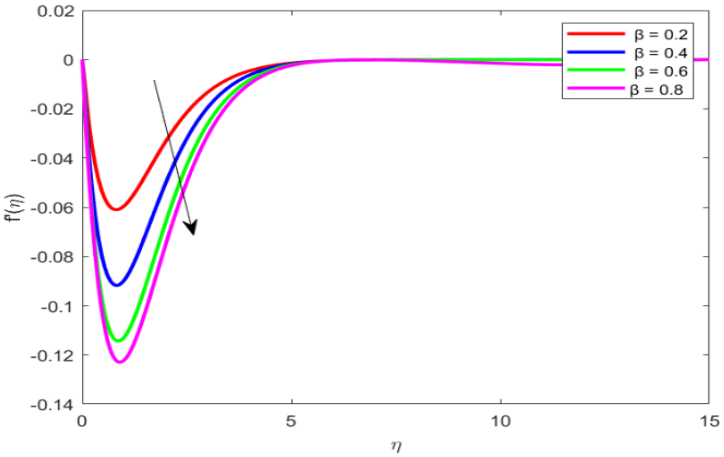

Fig. 4. Effect of porous parameter β on velocity profiles

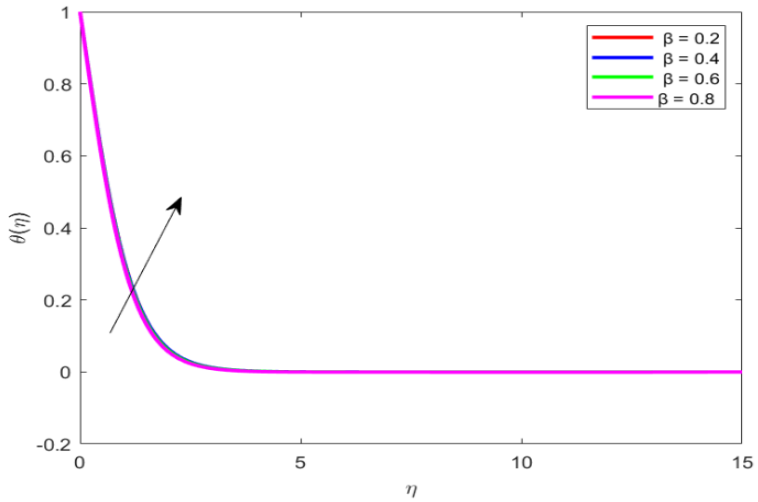

Fig. 5. Effect of β on temperature profiles

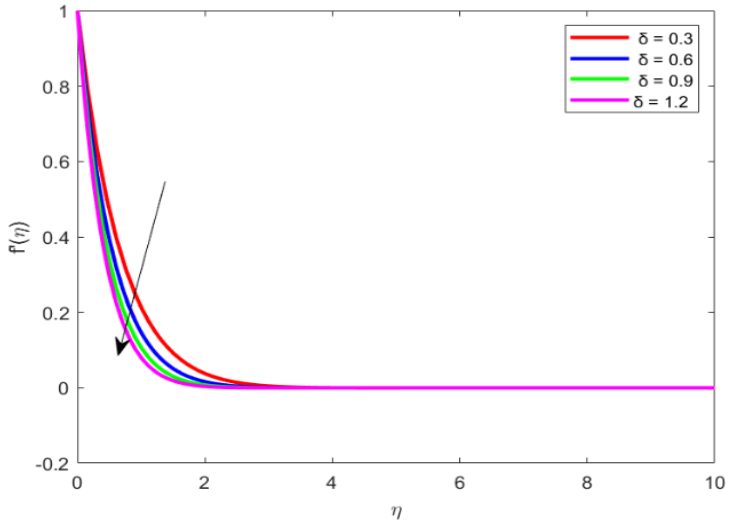

Fig. 6. Effect of unsteady parameter δ on velocity profiles

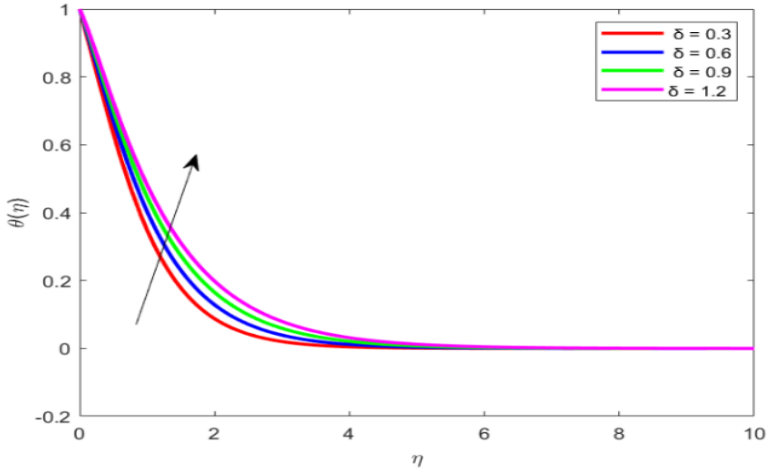

Fig. 7. Effect of unsteady parameter δ on temperature profiles

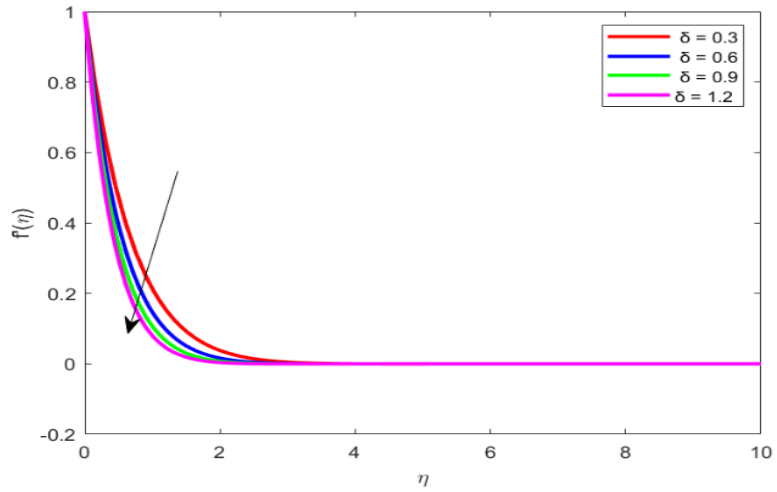

Fig. 8. Effect of unsteady parameter δ on concentration profiles

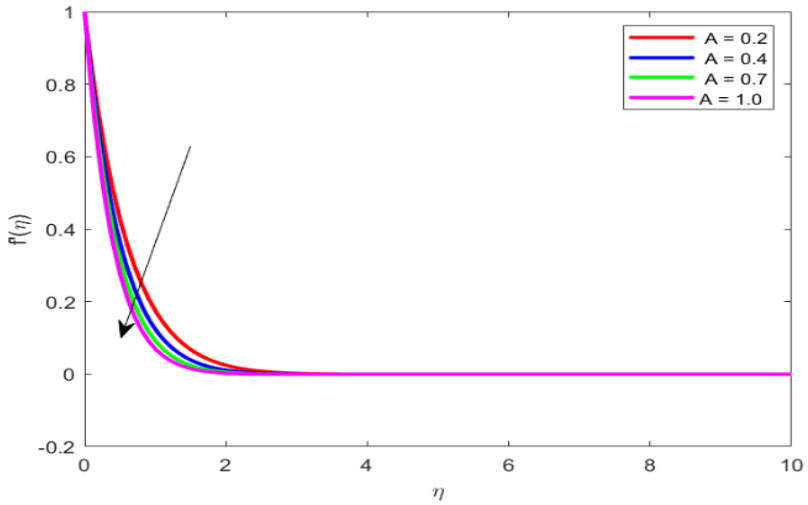

Fig. 9. Effect of Maxwell fluid parameter ʌ on velocity profiles

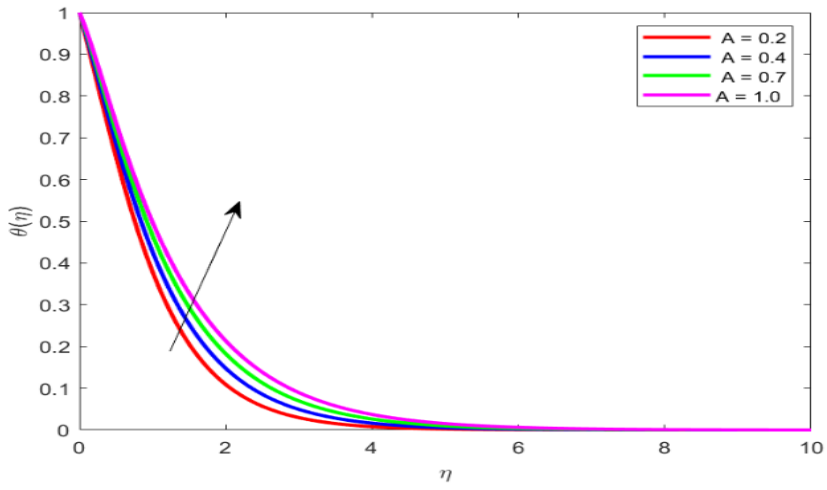

Fig. 10. Effect of Maxwell fluid parameter ʌ on temperature profiles

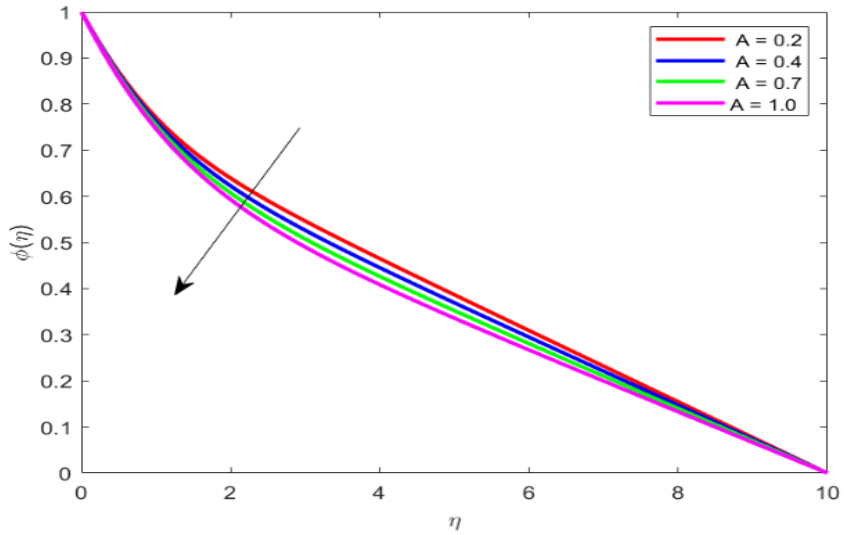

Fig. 11. Effect of Maxwell fluid parameter ∧ on concentration profiles

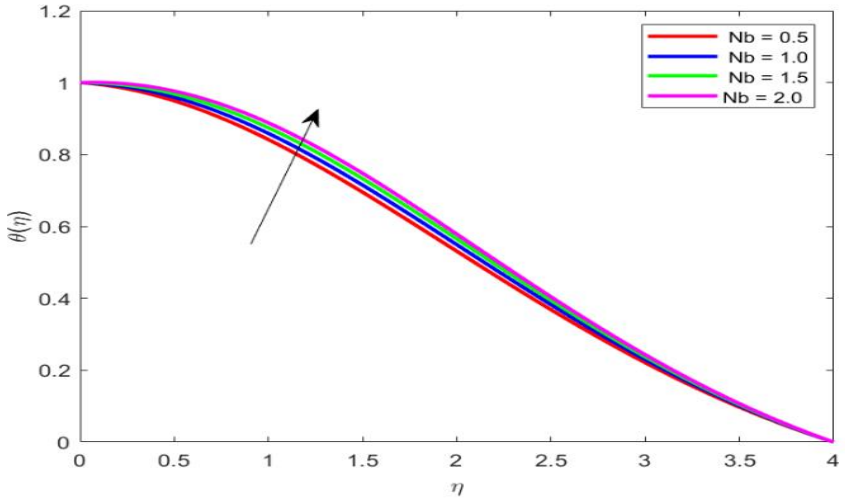

Fig. 12. Effect of Brownian motion parameter Nb on temperature profiles

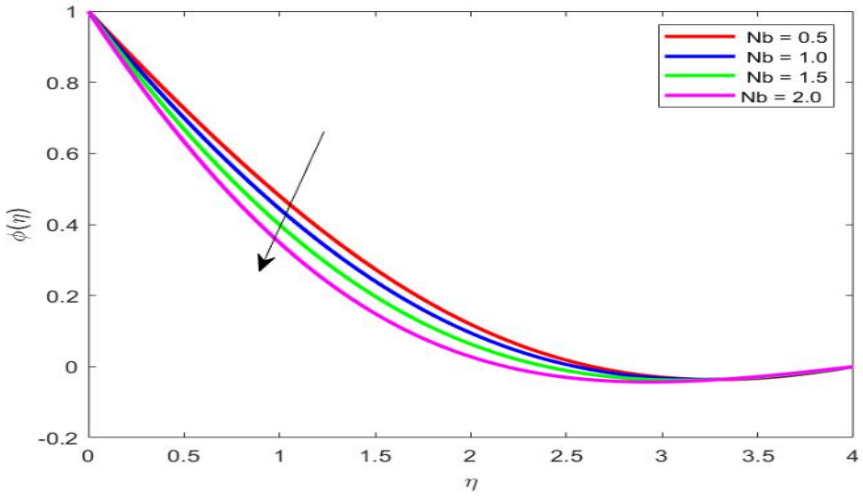

Fig. 13. Effect of Brownian motion parameter Nb on concentration profiles

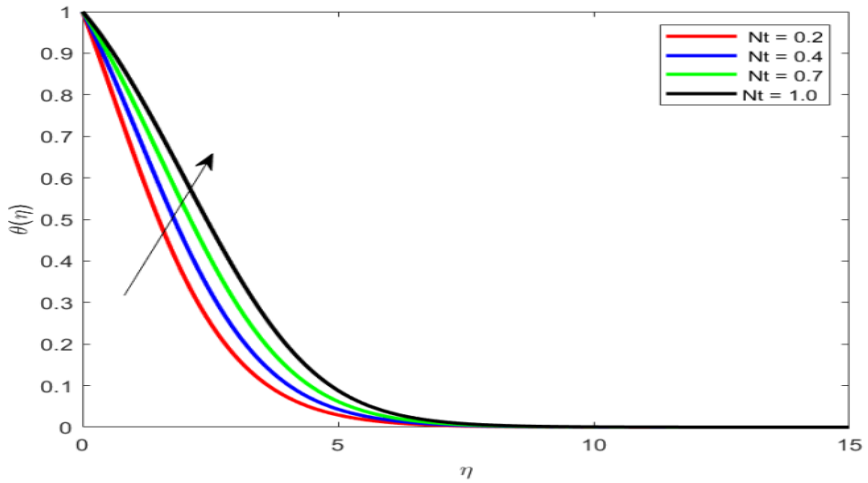

Fig. 14. Effect of Brownian motion parameter Nt on temperature profiles

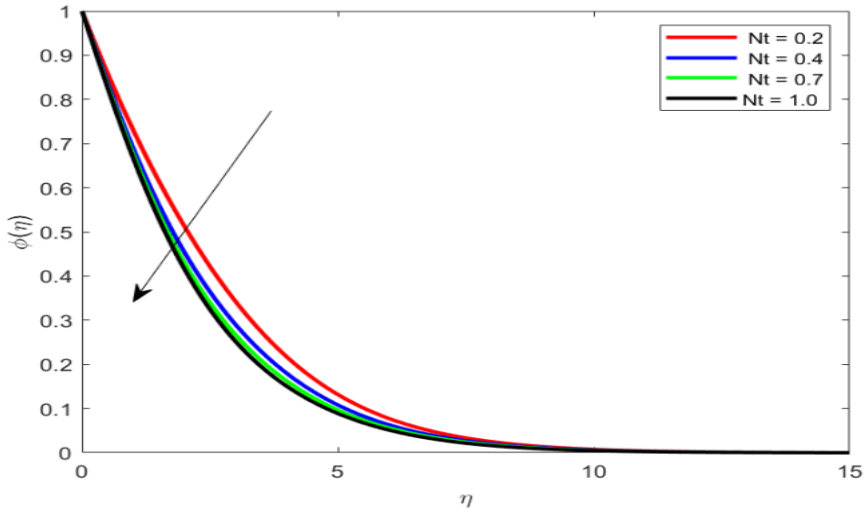

Fig. 15. Effect of Brownian motion parameter Nt on concentration profiles

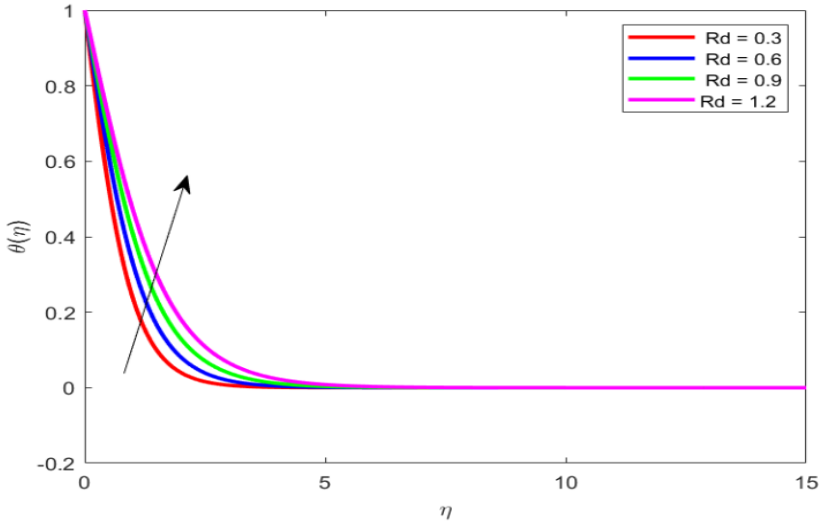

Fig. 16. Effect of Radiation parameter Rd on temperature profiles

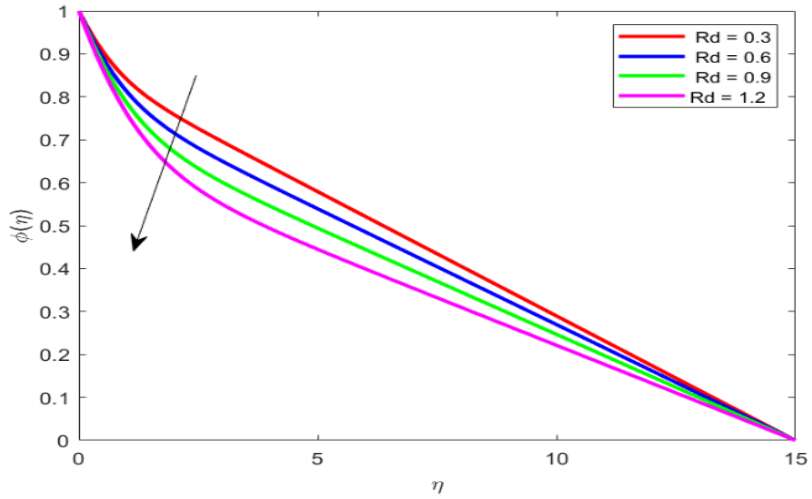

Fig. 17. Effect of Radiation parameter Rd on concentration profiles

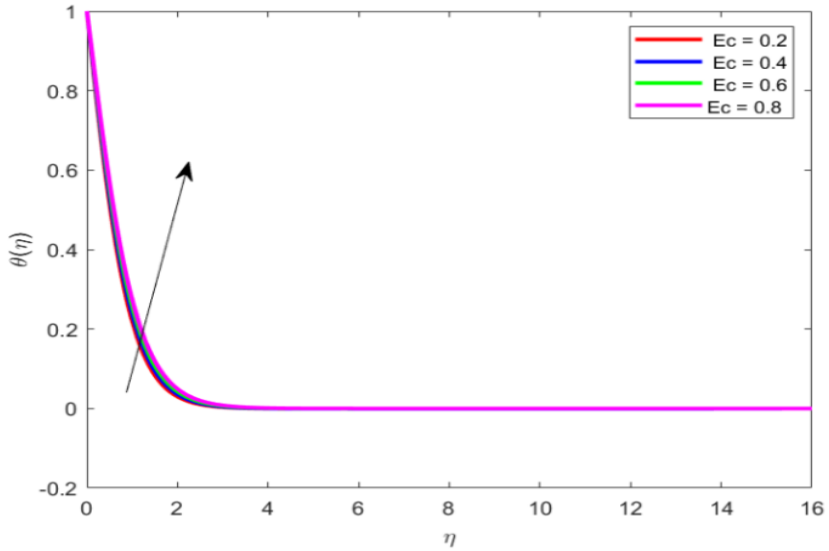

Fig. 18. Effect of Ekert number Rd on temperature profiles

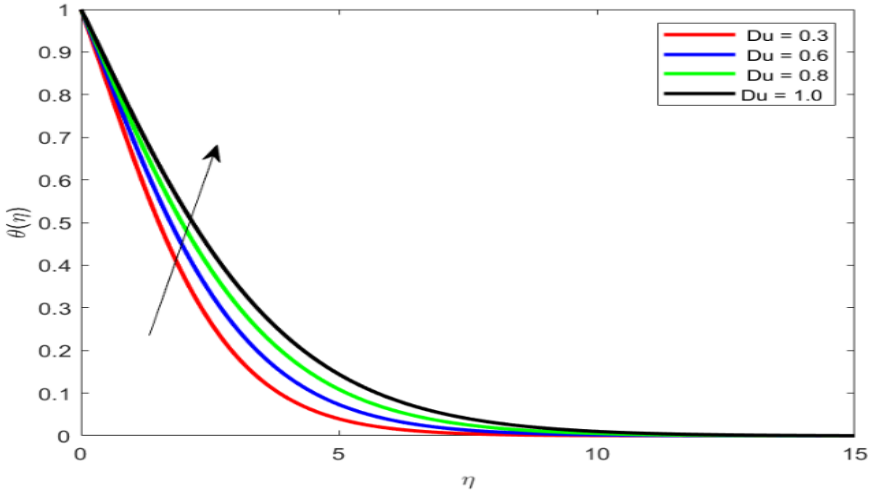

Fig. 19. Effect of diffusion thermo Parameter Du on temperature profiles

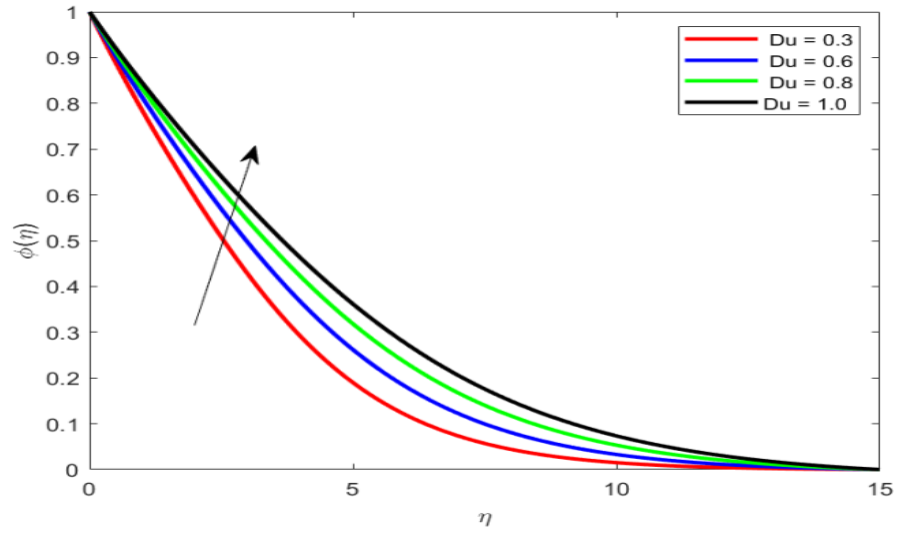

Fig. 20. Effect of diffusion thermo parameter Du on concentration profiles

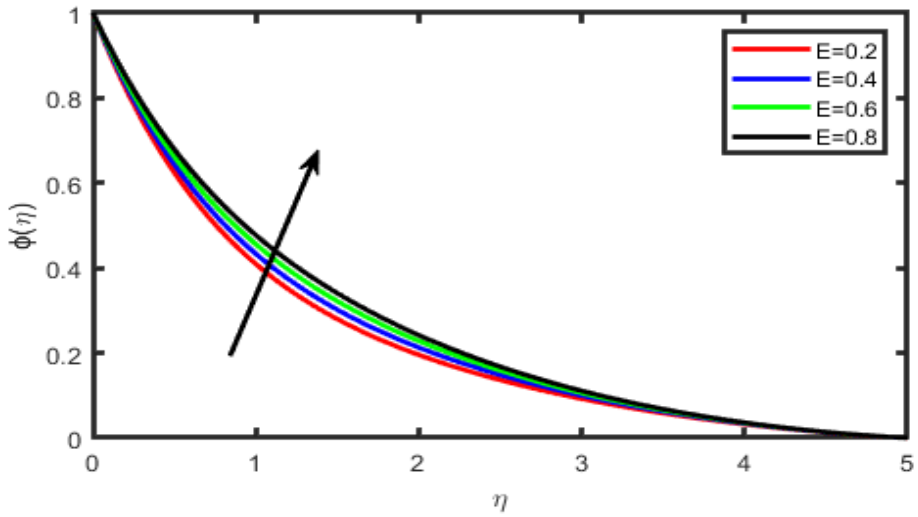

Fig. 21. Effect of activation energy parameter E on concentration profiles

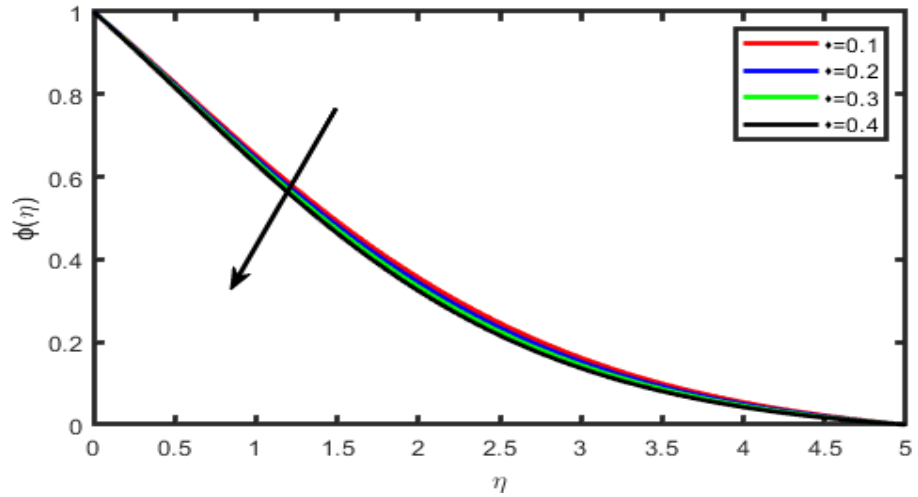

Fig. 22. Effect of rate chemical reaction parameter σon concentration profiles

Table 1
Comparison of skin friction coefficient $f''(0)$ for different values of M when ∧=E=σ=0

M	Venkata Ramudu *et al.,* [15]	Present Study
0.5	-0.376895	-0.37698
1.0	-0.529305	-0.529386
1.5	-0.654598	-0.654587

Table 2
Computation of $\mathrm{Re}_x^{1/2} Cf_x$, $\mathrm{Re}_x^{-1/2} Nu_x$ and $\mathrm{Re}_x^{-1/2} Sh_x$ for different parameters

Nb	Nt	Sc	Rc	Du	E	M	∧	$\mathrm{Re}_x^{1/2} Cf_x$	$\mathrm{Re}_x^{-1/2} Nu_x$	$\mathrm{Re}_x^{-1/2} Sh_x$
						1		1.11322	0.89745	0.25987
						2		1.44224	0.76264	0.65293
						3		1.87707	0.54094	0.98292
0.5								1.65587	0.82473	0.73298
1.0								1.18856	0.72936	0.98028
1.5								0.99846	0.56937	1.35282
	0.2							1.24847	0.98610	0.36927
	0.4							1.42984	0.76463	0.10828
	0.7							1.62846	0.53475	0.09282
		0.5						1.10947	0.11373	0.12228
		1.0						1.35847	0.10027	0.11383
		1.5						1.71947	0.08284	0.21282
			0.5					1.25847	0.11945	0.21293
			1.0					1.49948	0.10819	0.21292
			1.5					1.82944	0.07487	0.30292
				0.3				1.00048	0.71193	0.37282
				0.6				1.04948	0.68928	0.29298
				0.8				1.09948	0.65194	0.27292
					0.2			0.94094	0.87194	0.27228
					0.4			0.72948	0.81393	0.46292
					0.8			0.47948	0.78383	0.67292
							0.2	1.51837	0.10394	0.37292
							0.4	1.59933	0.09484	0.10292
							0.7	1.91948	0.04494	0.21292

6. Conclusion

In this work, investigated the effects of Thermal diffusion and Diffusion thermo on MHD mixed convective flow of Maxwell fluid past a porous vertical stretched surface in presence of thermal radiation and chemical reaction. The resulting partial differential equations, which describe the problem, are transformed in to ordinary differential equations by using introducing a similarity transformation and then solved by numerically by fourth order Runge-Kutta method along with shooting technique. Velocity, temperature and concentration profiles are presented graphically and analyzed. The findings of the numerical results can be summarized as follows:

- **i.** A stronger magnetic parameter M results in an increase in the temperature, concentration and transvers velocity
- **ii.** Thermal and concentration boundary layer thickness increase with the increase in thermophoresis parameter.

iii. Brownian motion parameter has opposite effect on temperature and concentration fields.
iv. The temperature distribution is a reducing function of thermal radiation Rd and Eckert number E
v. The fluid temperature enhances with increasing the Soretspecification.
vi. The concentration has opposite behavior with enhances Activation energy and rate of chemical reaction.

References

[1] Zierep, J., and Constantin Fetecau. "Energetic balance for the Rayleigh–Stokes problem of a Maxwell fluid." *International Journal of Engineering Science* 45, no. 2-8 (2007): 617-627.
[2] Fetecau, Corina, M. Athar, and Constantin Fetecau. "Unsteady flow of a generalized Maxwell fluid with fractional derivative due to a constantly accelerating plate." *Computers & Mathematics with Applications* 57, no. 4 (2009): 596-603.
[3] Renardy, Michael, and Xiaojun Wang. "Boundary layers for the upper convected Maxwell fluid." *Journal of Non-Newtonian Fluid Mechanics* 189 (2012): 14-18.
[4] Kodi, Raghunath, Ramachandra Reddy Vaddemani, M. Ijaz Khan, Sherzod Shukhratovich Abdullaev, Attia Boudjemline, Mohamed Boujelbene, and Yassine Bouazzi. "Unsteady magneto-hydro-dynamics flow of Jeffrey fluid through porous media with thermal radiation, Hall current and Soret effects." *Journal of Magnetism and Magnetic Materials* 582 (2023): 171033. https://doi.org/10.1016/j.jmmm.2023.171033.
[5] Raghunath, Kodi, Ravuri Mohana Ramana, Charankumar Ganteda, Prem Kumar Chaurasiya, Damodar Tiwari, Rajan Kumar, Dharam Buddhi, and Kuldeep Kumar Saxena. "Processing to pass unsteady MHD flow of a second-grade fluid through a porous medium in the presence of radiation absorption exhibits Diffusion thermo, hall and ion slip effects." *Advances in Materials and Processing Technologies* (2023): 1-18. https://doi.org/10.1080/2374068X.2023.2191450
[6] Suresh Kumar, Y., Shaik Hussain, K. Raghunath, Farhan Ali, Kamel Guedri, Sayed M. Eldin, and M. Ijaz Khan. "Numerical analysis of magnetohydrodynamics Casson nanofluid flow with activation energy, Hall current and thermal radiation." *Scientific Reports* 13, no. 1 (2023): 4021. https://doi.org/10.1038/s41598-023-28379-5
[7] Bafakeeh, Omar T., Kodi Raghunath, Farhan Ali, Muhammad Khalid, El Sayed Mohamed Tag-ElDin, Mowffaq Oreijah, Kamel Guedri, Nidhal Ben Khedher, and Muhammad Ijaz Khan. "Hall current and Soret effects on unsteady MHD rotating flow of second-grade fluid through porous media under the influences of thermal radiation and chemical reactions." *Catalysts* 12, no. 10 (2022): 1233. https://doi.org/10.3390/catal12101233.
[8] Deepthi, V. V. L., Maha MA Lashin, N. Ravi Kumar, Kodi Raghunath, Farhan Ali, Mowffaq Oreijah, Kamel Guedri, El Sayed Mohamed Tag-ElDin, M. Ijaz Khan, and Ahmed M. Galal. "Recent development of heat and mass transport in the presence of Hall, ion slip and thermo diffusion in radiative second grade material: application of micromachines." *Micromachines* 13, no. 10 (2022): 1566. https://doi.org/10.3390/mi13101566.
[9] Ganjikunta, Aruna, Hari Babu Kommaddi, Venkateswarlu Bhajanthri, and Raghunath Kodi. "An unsteady MHD flow of a second-grade fluid passing through a porous medium in the presence of radiation absorption exhibits Hall and ion slip effects." *Heat Transfer* 52, no. 1 (2023): 780-806. https://doi.org/10.1002/htj.22716
[10] Raghunath, Kodi, and Ravuri Mohanaramana. "Hall, Soret, and rotational effects on unsteady MHD rotating flow of a second-grade fluid through a porous medium in the presence of chemical reaction and aligned magnetic field." *International Communications in Heat and Mass Transfer* 137 (2022): 106287.. https://doi.org/10.1016/j.icheatmasstransfer.2022.106287.
[11] Kodi, Raghunath, Mohanaramana Ravuri, Nagesh Gulle, Charankumar Ganteda, Sami Ullah Khan, and M. Ijaz Khan. "Hall and ion slip radiative flow of chemically reactive second grade through porous saturated space via perturbation approach." *Waves in Random and Complex Media* (2022): 1-17. https://doi.org/10.1080/17455030.2022.2108555
[12] Vaddemani, Ramachandra Reddy, Sreedhar Ganta, and Raghunath Kodi. "Effects of hall current, activation energy and diffusion thermo of MHD Darcy-Forchheimer Casson nanofluid flow in the presence of Brownian motion and thermophoresis." *Journal of Advanced Research in Fluid Mechanics and Thermal Sciences* 105, no. 2 (2023): 129-145. https://doi.org/10.37934/arfmts.105.2.129145
[13] Hsiao KL. "Combined electrical MHD heat transfer thermal extrusion system using Maxwell fluid with radiative and viscous dissipation effects. " *ApplThermEng* 112 (2017): 1281–8.
[14] Reddy, N. Keerthi, HA Kumara Swamy, and M. Sankar. "Buoyant convective flow of different hybrid nanoliquids in a non-uniformly heated annulus." *The European Physical Journal Special Topics* 230 (2021): 1213-1225.

[15] Venkata Ramudu, Ankalagiri Chinna, Kempannagari Anantha Kumar, Vangala Sugunamma, and Naramgari Sandeep. "Heat and mass transfer in MHD Casson nanofluid flow past a stretching sheet with thermophoresis and Brownian motion." *Heat Transfer* 49, no. 8 (2020): 5020-5037.
[16] Cheng, Ching-Yang. "Soret and Dufour effects on free convection heat and mass transfer from an arbitrarily inclined plate in a porous medium with constant wall temperature and concentration." *International Communications in Heat and Mass Transfer* 39, no. 1 (2012): 72-77.
[17] Hayat, Tasawar, Muhammad Ijaz Khan, Muhammad Waqas, and Ahmed Alsaedi. "Stagnation point flow of hyperbolic tangent fluid with Soret-Dufour effects." *Results in physics* 7 (2017): 2711-2717.
[18] Hayat, T., M. Mustafa, and I. Pop. "Heat and mass transfer for Soret and Dufour's effect on mixed convection boundary layer flow over a stretching vertical surface in a porous medium filled with a viscoelastic fluid." *Communications in Nonlinear Science and Numerical Simulation* 15, no. 5 (2010): 1183-1196.
[19] Postelnicu, Adrian. "Influence of a magnetic field on heat and mass transfer by natural convection from vertical surfaces in porous media considering Soret and Dufour effects." *International Journal of heat and mass transfer* 47, no. 6-7 (2004): 1467-1472.
[20] Kafoussias, N. G., and E. W. Williams. "Thermal-diffusion and diffusion-thermo effects on mixed free-forced convective and mass transfer boundary layer flow with temperature dependent viscosity." *International Journal of Engineering Science* 33, no. 9 (1995): 1369-1384.
[21] Raghunath, K., R. Mohana Ramana, V. Ramachandra Reddy, and M. Obulesu. "Diffusion Thermo and Chemical Reaction Effects on Magnetohydrodynamic Jeffrey Nanofluid Over an Inclined Vertical Plate in the Presence of Radiation Absorption and Constant Heat Source." *Journal of Nanofluids* 12, no. 1 (2023): 147-156. https://doi.org/10.1166/jon.2023.1923
[22] Raghunath, Kodi. "Study of heat and mass transfer of an unsteady magnetohydrodynamic (MHD) nanofluid flow past a vertical porous plate in the presence of chemical reaction, radiation and Soret effects." *Journal of Nanofluids* 12, no. 3 (2023): 767-776. https://doi.org/10.1166/jon.2023.1923
[23] K. Raghunath, G. Nagesh, V. Ramachandra Reddy, and M. Obulesu. "Unsteady MHD fluid flow past an inclined vertical porous plate in the presence of chemical reaction with aligned magnetic field, radiation, and Soret effects." *Heat Transfer* 51, no. 3 (2022): 2742-2760. https://doi.org/10.1002/htj.22423
[24] Vaddemani, Ramachandra Reddy, Raghunath Kodi, and Obulesu Mopuri. "Characteristics of MHD Casson fluid past an inclined vertical porous plate." *Materials Today: Proceedings* 49 (2022): 2136-2142. https://doi.org/10.1016/j.matpr.2021.08.328
[25] Kodi, Raghunath, Ramachandra Reddy Vaddemani, and Obulesu Mopuri. "Effects of radiation absorption and aligned magnetic field on MHD Cassion fluid past an inclined vertical porous plate in porous media." *Simulation and Analysis of Mathematical Methods in Real-Time Engineering Applications* (2021): 273-291. https://doi.org/10.1002/9781119785521.ch12
[26] Kodi, Raghunath, Charankumar Ganteda, Abhishek Dasore, M. Logesh Kumar, G. Laxmaiah, Mohd Abul Hasan, Saiful Islam, and Abdul Razak. "Influence of MHD mixed convection flow for maxwell nanofluid through a vertical cone with porous material in the existence of variable heat conductivity and diffusion." *Case Studies in Thermal Engineering* 44 (2023): 102875. https://doi.org/10.1016/j.csite.2023.102875